**Proceedings of the ASME 2010 Pressure Vessels & Piping Division / K-PVP Conference**
**PVP2010**
**July 18-22, 2010, Bellevue, Washington, USA**

**PVP2010-25839**

# TRI-AXIAL SHAKE TABLE TEST ON THE THINNED WALL PIPING MODEL AND DAMAGE DETECTION BEFORE FAILURE

**Izumi Nakamura**
National Research Institute for Earth Science and Disaster Prevention
Tsukuba, Ibaraki, Japan

**Akihito Otani**
IHI Corporation
Yokohama, Kanagawa, Japan

**Yuji Sato**
IHI Corporation
Yokohama, Kanagawa, Japan

**Hajime Takada**
Yokohama National University
Yokohama, Kanagawa, Japan

**Koji Takahashi**
Yokohama National University
Yokohama, Kanagawa, Japan

## ABSTRACT

In order to investigate the influence of degradation on dynamic behavior of piping systems and clarify the failure mode of piping systems with local wall thinning, tri-axial shake table tests using three-dimensional piping system models were conducted. The degradation used in this study was wall thinning at elbows and a tee, which was considered to be caused in piping systems due to the effects of aging. The test results show that the dominant frequency and the maximum response acceleration would be reduced due to the existence of wall thinning. Nondestructive inspections such as ultrasonic inspection tests and penetrant inspection tests were applied in the interval of the shake table test in order to detect the damage caused by the repeated shaking. As a result, nondestructive inspection methods would be useful for detecting the damage before the failure caused by the seismic load.

## INTRODUCTION

Pressurized piping systems used for an extended period may develop degradations such as wall thinning or cracks due to aging. In order to ensure the seismic safety of degraded piping systems under seismic events, it is important to estimate the effects of degradation on the dynamic behavior and to ascertain the failure modes and ultimate strength of piping systems with degradation through experiments and numerical analyses. The authors have conducted a series of experiments and analysis for this several years and investigate the ultimate strength and failure modes of both piping systems with or without degradation, and establish the analytical model to estimate the fatigue life of piping systems [1-4]. Through these experiments and analyses, it is understood that the failure mode of the piping systems with wall thinning under the seismic loads is mainly the fatigue failure accompanied by ratchet deformation. It is also understood that the dynamic response and failure behavior of piping systems are affected by the existence of wall thinning, though the existence of crack is not so influenced on the dynamic behavior of the piping system, and more investigations are needed to understand the failure behavior of piping systems with wall thinning.

In order to obtain the additional experimental data of seismic behavior of piping system with wall thinning and to estimate the seismic safety margin of the piping systems, tri-axial shake table tests on 3-D piping system models were conducted. In the experiment, nondestructive inspection tests were attempted to detect the sign of pipe failure by the repeated shaking. In this paper, the summary of the shake table tests and nondestructive inspection results are described.

## PIPING SYSTEM TEST

### Model configuration

The configuration of the piping system model is shown in Fig.1. The model has six elbows and one tee, and two 756kg weights. The support conditions are three rigid anchors at every extremity of the pipe, a U-plate in the middle of the standpipe from Anchor3, and a ball bearing support under Weight1. The following two types of models were used for the shake table test;

1. Model name: AP3_A31

Condition of the defect: No defect

2. Model name: AP3_C31
   Condition of the defect: Full circumferential wall thinning at the tee and all elbows except for Elbow6

The pipe used for the test models was mainly carbon steel JIS STPT370 (Japanese industrial standards: carbon steel pipes for high temperature service), 100Asch80. That is, the outer diameter and the wall thickness of the pipe were 114.3mm and 8.6mm, respectively. The mean radius of curvature of the elbow was 152.4mm. Thinned wall elbows and tee were modeled by using thinner pipes, and carbon steel FSGP pipes for those parts. FSGP pipes are mainly used for gas or water pipelines in Japan. The nominal wall thickness of 100A FSGP pipe was 4.5mm, so the wall thinning ratio came to 48%.

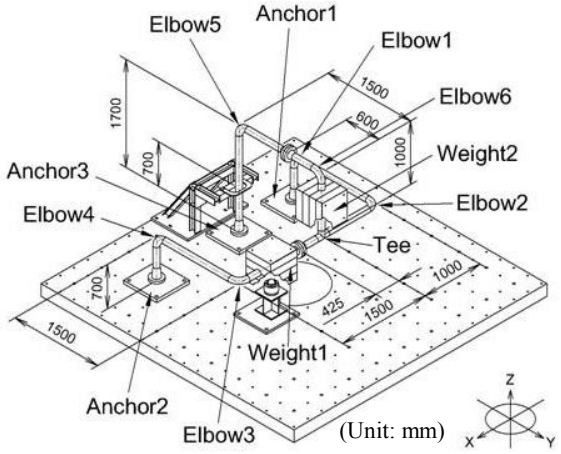


Mass of Weight1 and Weight2: 756kg

**Fig.1 Configuration of the test model**

Figure 2 shows the vibration modes and natural frequencies of the test model AP3_A31 (without wall thinning). The dominant frequencies at the first mode were calculated as 4.63Hz for AP3_A31 and 3.49Hz for AP3_C31. The dominant deformation of this mode is the translational motion in X direction as Elbow2 and Elbow3 were deformed in in-plane bending and Elbow1 and Elbow4 were deformed in out-of-plane bending. The model names and the conditions of wall thinning are summarized in Table 1.

## Input condition

The tri-axial shake table of IHI was used for the excitation tests. The excitation wave was originally recorded at JMA Suttsu in the 1993 South-west off Hokkaido Earthquake. Considering the capacity of the shake table, the original recorded wave was filtered by 1.5Hz high-pass filter. Hereinafter the filtered seismic motion was referred to just as "Suttsu HPF". The seismic motion was selected from the viewpoint that the dominant frequency was close to the model's

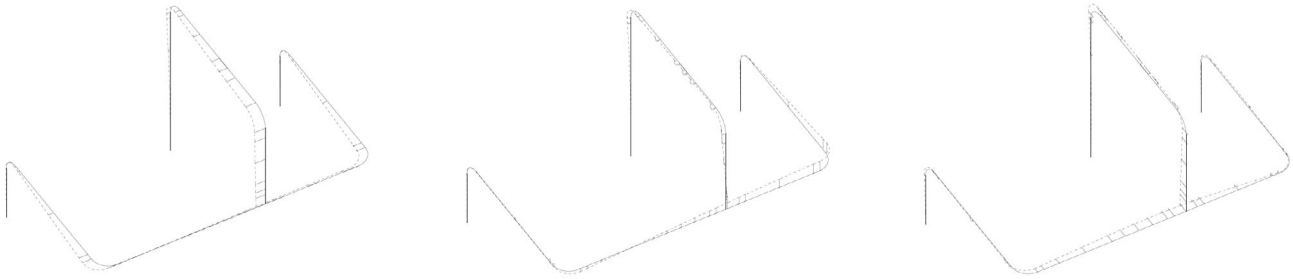

1st mode: 4.63Hz  2nd mode: 7.45Hz  3rd mode: 12.08Hz

**Fig.2 Vibration modes of the piping system model without wall thinning (AP3_A31)**

**Table 1 Model characteristics**

| Name | Material at pipe joint | $S_y$[MPa]* | $S_u$[MPa]* | $S_m$[MPa]* | Condition of wall thinning | Internal pressure [MPa] |
|---|---|---|---|---|---|---|
| AP3_A31 | STPT370 | 215 | 370 | 125 | No defect | 3 |
| AP3_C31 | FSGP (Thinned wall pipe joints) | 147 | 290 | - | Full circumferential thinning<br>Depth: $0.48t$**<br>Wall thinning parts:<br>Elbow1, Elbow2, Elbow3, Elbow4, Elbow5, and Tee | |

* Values determined by the design code [5]. $S_m$ of FSGP is not determined in the code.
** "$t$" denotes the nominal wall thickness of 100Asch80.

dominant frequency, and that the duration of the seismic motion was comparatively long to cause the fatigue failure effectively by the excitation tests. In the experiment, the EW component was input to X direction of the shake table shown in Fig.1, the NS component to Y direction, the UD component to Z direction. The input acceleration time histories and the acceleration response spectrum are shown in Fig.3. A wide band spectrum random wave (2~30Hz) and sinusoidal waves were also used in the excitation tests. The test models were pressurized to 3MPa by ambient temperature water. The tests were performed mainly by Suttsu HPF in various acceleration levels until the failure was caused on the model. Here, the failure of the model was determined by the leak of pressurized water. The primary stress intensities under 100% Suttsu HPF calculated by spectrum analysis are listed in Table 2. As shown in Table 2, the maximum primary stress intensity is about $3.3S_m$ at Elbow3 for AP3_A31. The maximum stress intensity by 100% Suttsu HPF on AP3_A31 is very close to the primary stress limit of $3S_m$ for the class 1 piping in the previous Japanese seismic code [6], which was revised in 2008 and whose limitation of the primary stress intensity was removed. The maximum stress intensity calculated by SRSS of X, Y, and Z excitation was predicted to occur at Elbow3 as for AP3_A31 and at Tee as for AP3_C31.

## Measurement

The following data were recorded with 1024Hz sampling frequency.

(1) Input acceleration of the shake table in three directions.
(2) Response acceleration of the test models at elbows and weights.
(3) Opening-closing in-plane displacement of Elbow2 and Elbow3.
(4) Strain at the outer surface of elbows, tee, and straight pipes next to these pipe joints.
(5) Internal pressure

The measurement method using image processing technique [7] was also used to measure the overall deformation of the test models. The outer diameters of the elbows and the tee were also

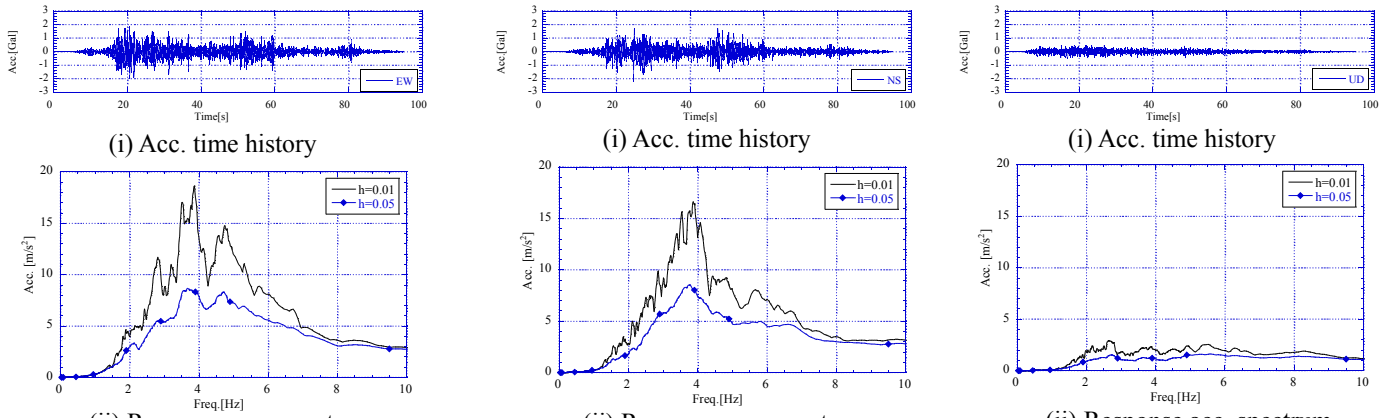


(i) Acc. time history (i) Acc. time history (i) Acc. time history

(ii) Response acc. spectrum (ii) Response acc. spectrum (ii) Response acc. spectrum

(a) EW (X) (b) NS (Y) (c) UD (Z)

**Fig.3 Acceleration time histories and response acc. spectrum (*h*: damping ratio)**

**Table 2 Primary stress intensities caused by 100% Suttsu HPF calculated by design analysis**

| | AP3_A31 | | AP3_C31 | |
|---|---|---|---|---|
| | Primary stress intensity [MPa] | Ratio to $S_m$ | Primary stress intensity [MPa] | Ratio to $S_m$ |
| Elbow1 | 409 | 3.27 | 1095 | 8.76 |
| Elbow2 | 348 | 2.79 | 783 | 6.26 |
| Elbow3 | 410 | 3.28 | 849 | 6.79 |
| Elbow4 | 387 | 3.10 | 1060 | 8.48 |
| Elbow5 | 179 | 1.43 | 693 | 5.54 |
| Elbow6 | 296 | 2.37 | 468 | 3.74 |
| Tee | 364 | 2.92 | 1274 | 10.2 |

* $S_m$=125[MPa], determined by the design code [5].

measured with a vernier caliper at some intervals of excitation tests.

## TEST RESULT

### Result of the excitation tests

The excitation tests and the results are summarized in Table 3. The test models were excited by a wide band spectrum random wave in each direction at 0.5m/s$^2$~ 1.5m/s$^2$. As for AP3_A31, the excitation test by the random wave in X direction at 2.0m/s$^2$ was also conducted. Table 4 shows the dominant frequencies and the damping ratios at the first mode obtained by the excitation test in X direction and the modal analysis results obtained before the excitation tests. The damping ratio written at "Analysis" column in Table 4 is the value to use in the seismic design of piping systems in Japan [6]. As shown in Table 4, the dominant frequencies by the experiments were higher than those by the analytical results. They had a tendency to come down as the input acceleration level was raised. The reason of the tendency is considered to come from the friction

**Table 4 Dominant frequency and damping ratio at the 1st mode**

| | | Experiment | | | Analysis |
|---|---|---|---|---|---|
| | | Max. Input acc. of random wave | | | |
| | | 0.5m/s$^2$ | 1.0m/s$^2$ | 1.5m/s$^2$ | |
| AP3_A31 | *f* | 6.17Hz | 5.18Hz | 5.30Hz | 4.63Hz |
| | *h* | 0.018 | 0.017 | 0.012 | 0.005 |
| AP3_C31 | *f* | 4.52Hz | 4.20Hz | 3.99Hz | 3.49Hz |
| | *h* | 0.018 | 0.009 | 0.022 | 0.005 |

* *f*: dominant frequency, *h*: damping ratio

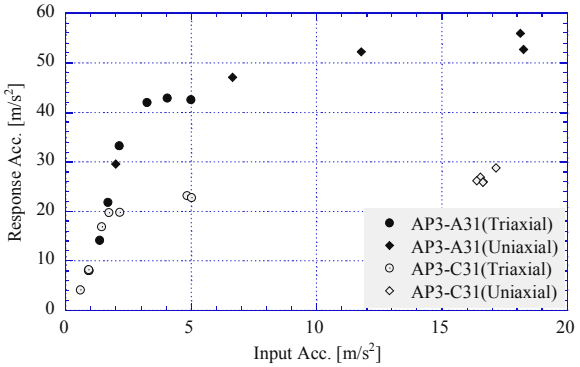


**Fig.4 Relation between input and response acc. at Weight 2**

**Table 3 Test results**

| Name | Wall thinning condition | Contents of the excitation | | | Test results |
|---|---|---|---|---|---|
| | | Waveform | Max. acc. or magnification to the original waveform | Number of input times | |
| AP3_A31 | No defect | Random (X, Y, Z)* | 0.5m/s$^2$, 1.5m/s$^{2**}$ | 1 for each | Fatigue failure at Elbow3 during the second excitation by the sinusoidal wave |
| | | Random (X)* | 1.0m/s$^2$, 2.0m/s$^{2**}$ | | |
| | | Suttsu HPF (X+Y+Z) | 40%, 60%, 80%, 100% 150%, 200%, 250% | | |
| | | Suttsu HPF (X) | 100%, 300%, 500%, | | |
| | | | 750% | 2 | |
| | | Sinusoidal 4.5Hz, 40sec | 9.8m/s$^2$ | 2 | |
| AP3_C31 | Wall thinning at elbows and tee except for Elbow6 | Random (X, Y, Z)* | 0.5m/s$^2$, 1.0m/s$^{2**}$ | 1 for each | Fatigue failure at Elbow1 after the second excitation by the sinusoidal wave |
| | | Random (X)* | 1.5m/s$^{2**}$ | | |
| | | Suttsu HPF (X+Y+Z) | 20%, 40%, 60%, 80%, 100% | | |
| | | | 250% | 2 | |
| | | Suttsu HPF (X) | 750% | 5 | |
| | | Sinusoidal 3.2Hz, 40sec | 9.8m/s$^2$ | 2 | |

* "Random wave" is the wide band spectrum random wave with the spectrum band of 2 – 30Hz.
** The acceleration is the max. peak acceleration of the input wave.

at the pipe supports. The damping ratios also came down as the input acceleration level was raised, and this result also indicates that the friction affects the piping systems' dynamic response especially when the input acceleration level is relatively low. The dominant frequencies of AP3_C31, the model with wall thinning, were lower than those of AP3_A31, the model without wall thinning. Referring to the experimental result by the excitation of 1.5m/s2 input acceleration, the reduction rate of 3D_C31 to 3D_A31 in the dominant frequency is about 25%, equal in both the experiment and analysis results, though the values of the dominant frequencies themselves by the analysis are different from those by the experiment. The damping ratios by the experiments were higher than 0.5%, which was used in the seismic design as a whole.

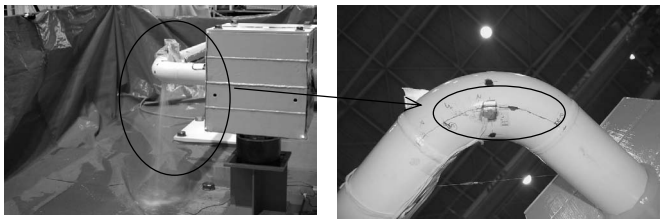

(a) AP3-A31 (at Elbow 3)

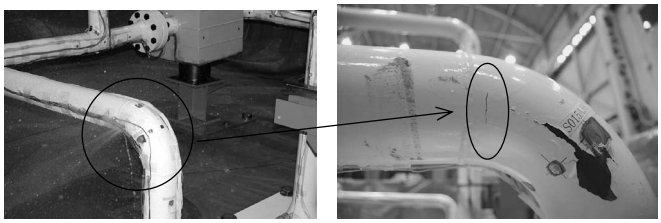

(b) AP3-C31 (at Elbow 1)

**Fig.5 Failure modes of test models**

After the excitation by the random wave, the models were excited by 40% ~ 250% magnifications of Suttsu HPF in three directions, and then, the magnification was raised up to 750% only in X directional shaking (EW component of the seismic motion). These limits of the magnification of three directional shaking and X directional shaking were determined by the ability of the shake table. Figure 4 shows the relation between the input acceleration and the response acceleration measured at Weight2 in X direction. In Fig.4, the solid marks denote the result of AP3_A31, and the open marks denote the result of AP3_C31. The circle marks are the results by tri-axial shaking tests, and the diamond marks are the results by uniaxial shaking tests. As shown in Fig.4, AP3_A31 responded in elastic region until about 2.1m/s$^2$ of the input acceleration (100% Suttsu HPF), and AP3_C31 responded in the elastic region about 1.7m/s$^2$ of the input acceleration (80% Suttsu HPF). The response acceleration level of AP3_C31 was lower than that of AP3_A31, and the decreasing ratio was about 50% of AP3_A31. The lower response accelerations of AP3_C31

**Table 5 Schedule of excitation and nondestructive inspection**

| | Excitation condition | Nondestructive inspection |
|---|---|---|
| AP3_A31 | | UT(#01) and DRT, before the excitation |
| | Random, X,Y,Z, 0.5~1.5m/s$^2$ | |
| | Random, X, 2.0m/s$^2$ | UT(#02) after the excitation |
| | Suttsu HPF, X+Y+Z 40%~100% | UT(#03) and DRT after the 100% excitation |
| | Suttsu HPF, X 100% | |
| | Suttsu HPF, X+Y+Z 150%~250% | UT(#04) after the 250% excitation |
| | Suttsu HPF, X, 300%, 500%, 750%(twice) | |
| | Sinusoidal 4.5Hz 9.8m/s$^2$ (twice) – pipe failed | UT(#05), DRT, PT, MT after the failure |

| | Excitation condition | Nondestructive inspection |
|---|---|---|
| AP3_C31 | | UT(#06) and DRT, before the excitation |
| | Random, X,Y,Z, 0.5~1.0m/s$^2$ | |
| | Random, X, 1.5m/s$^2$ Suttsu HPF, X+Y+Z 20%~100% | UT(#07) after the 60% excitation, UT(#08) after the 100% excitation |
| | Suttsu HPF, X+Y+Z 250%(twice) | UT(#09) and DRT after the second 250% excitation |
| | Suttsu HPF, X, 750%(fifth) | UT(#10) after the first excitation, UT(#11) after the second excitation, UT(#12) after the third excitation |
| | Sinusoidal 3.2Hz 9.8m/s$^2$ | DRT after the excitation |
| | Sinusoidal 3.2Hz 9.8m/s$^2$ (second excitation, pipe failed)) | UT(#13), DRT, PT, MT after the failure |

compared with those of AP3_A31 is considered due to the larger plastic deformation caused on the thinned wall pipe joints. The larger plastic deformation increased the damping ratio and decreased the dominant frequency of the test model. The model came into the lower response region of the response spectrum in Fig. 3 because of these effects. The difference of the response between the tri-axial shaking and the uniaxial shaking was not so remarkable in the relation between the input acceleration and the response acceleration. More investigation is necessary to clarify the difference of the response under tri-axial shaking and that of uniaxial shaking.

**Table 6 UT result of AP3_A31**

| | UT performance numbers* | | | | |
|---|---|---|---|---|---|
| | #01 | #02 | #03 | #04 | #05 |
| Elbow1 | – | – | – | – | – |
| Elbow2 | Indicated (1) | Indicated (1) | Indicated (1) | Indicated (1) | Indicated (1) |
| Elbow3 | – | – | Indicated (4) | Indicated (4)** | Indicated (6)** |
| Elbow4 | – | – | – | – | Indicated (1) |
| Elbow5 | – | Indicated (3) | Indicated (3) | Indicated (5) | Indicated (5) |
| Elbow6 | – | – | – | – | – |
| Tee | – | – | – | – | – |

The numbers in blankets are the number of indicated defects.
* Performance numbers of UT correspond to the numbers written in Table 5.
** The four indicate defects linked each other, but the number of indicated defects was listed by the original number.

## Failure mode and nondestructive inspection during the excitation tests

Because the failure did not occur on both test models by the excitation of 750% Suttsu HPF, the excitations by a sinusoidal wave were conducted. The failure mode of AP3_A31 was the fatigue failure at the flank of Elbow3 which was subjected to in-plane bending. The failure mode of AP3_C31 was the fatigue failure at the neighbor of the weld at Elbow1 which was subjected to out-of-plane bending. Figure 5 shows the failure mode of these test models. The failure mode was the fatigue failure accompanied by the ratchet deformation, like as the failure mode obtained by the past research programs [1, 3]. The amount of the ratchet deformation was about less than 1% as for AP3_A31 and more than 8% as for AP3_C31.

In the experiment, nondestructive inspections were conducted on the test models at some intervals during the excitations and on the cut-off pipe joints after the series of excitations. The objective of the nondestructive inspections was to try to detect the sign of the failure by the repeated shaking before a through-wall crack caused on the pipe. The applied nondestructive inspection methods were as follows;

(1) Inspections during the excitations:
  1) Ultrasonic testing (UT)
  2) Digital radiographic testing (DRT)

**Table 7 UT result of AP3_C31**

| | UT performance numbers* | | | | | | | |
|---|---|---|---|---|---|---|---|---|
| | #06 | #07 | #08 | #09 | #10 | #11 | #12 | #13 |
| Elbow1 | – | – | – | – | – | – | – | Indicated (1) |
| Elbow2 | – | – | – | – | – | – | Indicated (1) | Indicated (4) |
| Elbow3 | – | – | – | Indicated (1) | Indicated (2) | Indicated (2) | Indicated (4) | Indicated (4) |
| Elbow4 | – | – | – | – | – | – | – | – |
| Elbow5 | – | – | Indicated (2) | Indicated (2) | Indicated (3) | Indicated (3) | Indicated (3) | Indicated (3) |
| Elbow6 | – | – | – | Indicated (1) | Indicated (1) | Indicated (1) | Indicated (1) | Indicated (1) |
| Tee | – | – | – | – | – | – | – | – |

The numbers in blankets are the number of indicated defects.
* Performance numbers of UT correspond to the numbers written in Table 5.

(2) Inspections after the series of the excitations:
    1) Liquid penetrant testing (PT)
    2) Magnetic particle testing (MT)

These nondestructive inspection methods are commonly used method in the field. Because UT and DRT were conducted to detect the defect caused on the body of the pipe joint, the inspections were performed at the body of the pipe joint, not at the weld line. Sensors such as accelerometers, strain gages, and cables of them remained on the pipe models, and the coating materials were not removed when UT and DRT were performed. So there were some parts of the pipe joints where UT could not be performed due to the remained sensors, or where DRT could not distinguish the defect due to the overlap of the cables.

The schedule of the excitation tests and the nondestructive inspections are listed in Table 5. The results of UT are listed in Table 6 as for AP3_A31 and in Table 7 as for AP3_C31. In Tables 6 and 7, the performance numbers of UT correspond to the numbers written in Table 5. As shown in Table 6, a defect was detected at Elbow2 of AP3_A31 when UT was conducted before the excitation tests. But the defect did not develop by the excitation. The defects detected at Elbow5 of AP3_A31 after the excitation of the $2m/s^2$ random wave did not develop by following excitations either. On the other hand, the defects with the length of 5~35mm were detected at Elbow3 of AP3_A31 after the excitation of 100% Suttsu HPF, and the defects developed and linked together by following excitations. The failure of the pipe, which was defined by the crack penetration in the experiments, was finally caused from the defect in AP3_A31. Though the defect at Elbow3 after the whole excitations was detected by DRT, defects before failure were not detected by DRT. Figure 6 shows the result of DRT at Elbow2 and Elbow3 after all the excitations for AP3_A31.

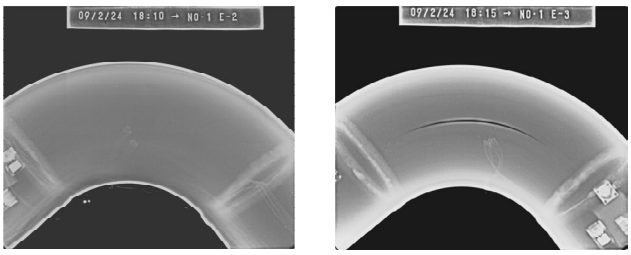


(a) Elbow 2 (b) Elbow 3

**Fig.6 DRT result of AP3_A31**

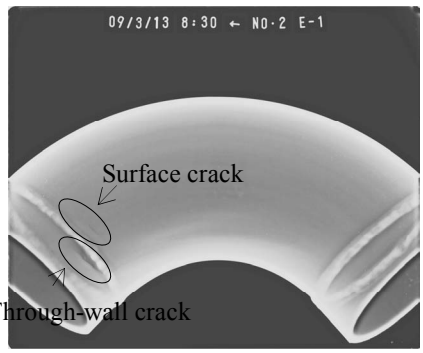


**Fig.7 DRT result of AP3_C31, Elbow1**

As for AP3_C31, defects were not detected by UT before the excitation. The defects were detected at Elbow5 after the excitation of 100% Suttsu HPF, at Elbow3 after the second excitation of 250% Suttsu HPF, at Elbow6 after the first excitation of 750% Suttsu HPF, and at Elbow2 after the third excitation of 750% Suttsu HPF. The defects at Elbow3 and Elbow5 detected in the middle of the excitation tests developed by following excitations. Though the failure was caused finally at Elbow1, defects were not detected at Elbow1 by UT. Though the crack was caused at the position where the sensor cables were obstacles to the inspection, it cannot be determined whether the defect at Elbow1 was not caused just before the failure, or the inspection was impossible due to the cables as a practical matter. A surface crack at Elbow1 on the other side of the pipe where the through-wall crack appeared was detected by DRT after the whole excitations, but other defects before failure were not detected by DRT. In AP3_C31, the maximum primary stress was estimated to occur at Tee as shown in Table 2. Though a remarkable ratchet deformation was observed at Tee, no defect was detected by UT or DRT in actual piping system model. Figure 7 shows the result of DRT at Elbow1 after the whole excitations for AP3_C31.

As for the inspections after the whole excitations on the cut-off pipe joints, defects were detected at Elbow2 and Elbow3 of AP3_A31 by PT, and detected at Elbow1, Elbow2, Elbow3, and Elbow6 of AP3_A31 by MT. For AP3_C31, defects were detected at Elbow1, Elbow3, Elbow5, and Elbow6 by PT, and detected at Elbow1, Elbow3, and Elbow6 by MT. The results of MT and PT are listed in Table 8. Compared with the results between the different inspection methods, the detection of the defects depended on the inspection methods and there was some difference in the result of the inspection, for example, a defect was detected at Elbow2 of AP3_C31 by UT during the

**Table 8 The result of MT and PT**

| | AP3_A31 | | AP3_C31 | |
|---|---|---|---|---|
| | PT | MT | PT | MT |
| Elbow1 | – | Indicated | Indicated | Indicated |
| Elbow2 | Indicated | Indicated | – | – |
| Elbow3 | Indicated | Indicated | Indicated | Indicated |
| Elbow4 | – | – | – | – |
| Elbow5 | – | – | Indicated | – |
| Elbow6 | – | Indicated | Indicated | Indicated |
| Tee | – | – | – | – |

excitation tests, but not detected by PT and MT after the excitation tests. MT seems to be the most sensitive method to detect the defects, and then, UT, PT, and DRT in order. The result of UT agreed well with the result of MT. As shown in Tables 6 and 7, a defect was detected by UT though the test model was not subjected to the excitation tests, and some defects were detected on the elbows on which the applied stress was not so high. These defects were considered as the scars by the production process of pipe joints. However, UT also detected the defects which finally caused the pipe failure at an early stage of the excitation at Elbow3 of AP3_A31. Considering the inspection results, UT may be a useful inspection method to detect the sign of failure by seismic loads, though it sometimes detects nonrelevant indications.

## CONCLUSION

Shake table tests on three-dimensional piping system models with thinned wall pipe joints were conducted to investigate the influence of degradation on dynamic behavior of piping systems. The results show that the dominant frequency and the maximum response acceleration would be reduced due to the existence of wall thinning, but the reduction rate of the dominant frequency can be predicted by the analytical method used in the design. The failure mode of the piping system models were fatigue failure, and a remarkable ratchet deformation was also observed on the failed part for the model with wall thinning. In the experiments, nondestructive inspections were applied to detect the damage caused by the repeated shaking. As a result, UT may be a useful inspection method to detect the damage before failure by seismic load, though it sometimes detects nonrelevalnt indications.

## ACKNOWLEDGMENTS

This study is the result of "A research program on the quantitative estimation of the seismic safety capacity of thinned wall piping systems" carried out under the Strategic Promotion Program for Basic Nuclear Research by the Ministry of Education, Culture, Sports, Science and Technology, Japan. The authors wish to extend their appreciation to the organization for funding and supporting this research program. For conducting the research program, the study groups named "Study group for Aged Piping, the Third stage"(AP3 study group) are organized. The authors are grateful to members of the study group for their useful discussions and suggestions on the planning and the evaluation of the experiment results. The seismic motion used in the experiment was originally recorded by JMA. The authors are also grateful to them.

## REFERENCES

[1] Nakamura, I., Otani, A., and Shiratori, M., 2004, "Failure behavior of piping systems with wall thinning under seismic loading", Transactions of the ASME, Journal of Pressure Vessel Technology, **126**, pp.85-90.

[2] Mikami, A., Udagawa, M., and Takada, H., 2004, "Study on estimation method for seismic safety margin of 3D piping system with degradation – Establishing elasto-plastic analysis model –", ASME PVP **473**, pp.125-132.

[3] Nakamura, I., Otani, A., and Shiratori, M., 2007, "Comparison of failure modes of piping systems with wall thinning subjected to in-plane, out-of-plane and mixed mode bending under seismic load: an experimental approach", Proceedings of PVP2007, PVP2007-26497. (CD-R)

[4] Tsunoi, S., Mikami, A., Nakamura, I., Otani, A., and Shiratori, M., 2007, "Comparison of failure modes of piping systems with wall thinning subjected to in-plane, out-of-plane and mixed mode bending under seismic load: computational approach", Proceedings of PVP2007, PVP2007-26476.(CD-R)

[5] The Japan Society of Mechanical Engineers, 2005, "Codes for Nuclear power Generation Facilities – Rules on Design and Construction for Nuclear Power Plants –", JSME S NC1-2005. (in Japanese)

[6] Japan Electric Association, 1987, "Technical Guidelines for Aseismic Design of Nuclear Power Plants", JEAG4601-1987 (in Japanese)

[7] Fujita, S., Furuya, O., and Mikoshiba, T., 2004, "Research and development of measurement method for structural fracturing process in shake table tests using image processing technique", Transactions of the ASME, Journal of Pressure Vessel Technology, **126**, pp. 115-121